

Electroacoustic method for measuring air-flow resistivity in a standing wave tube

Alba, Jesús¹

**Universitat Politècnica de València, Campus de Gandia
C/ Paraninfo nº1, 46730 Grao de Gandia (Spain)**

Arenas, Jorge P.²

**Institute of Acoustics, Univ. Austral of Chile,
PO Box 567, Valdivia, Chile**

Del Rey, Romina³

**Universitat Politècnica de València, Campus de Gandia
C/ Paraninfo nº1, 46730 Grao de Gandia (Spain)**

Rodríguez, Juan Carlos⁴

**Universitat Politècnica de València, Campus de Gandia
C/ Paraninfo nº1, 46730 Grao de Gandia (Spain)**

ABSTRACT

Air-flow resistivity is a very important parameter for characterizing porous sound absorbing materials. A number of theoretical models are dependent on values of air-flow resistivity. Air-flow resistivity has also been used in the selection of materials for noise insulation and room acoustic applications. However, direct measure of air-flow resistivity is not simple. To overcome this problem, several indirect alternative methods have been proposed, such as the one proposed by Ingard & Dear in a standing wave tube. In this work, an electroacoustic procedure is proposed to determine this parameter from the method devised by Ingard & Dear. It is shown that, under certain conditions, the air-flow resistivity can be obtained from direct measurements of electric impedance.

Keywords: Airflow resistivity, Porous materials, Electroacoustics

I-INCE Classification of Subject Number: 72

¹ jesalba@fis.upv.es

² jprenas@uach.cl

³ roderey@fis.upv.es

⁴ juarodve@upv.es

1. INTRODUCTION

Most sound-absorbing materials, regardless of the material from which they were made of, are porous. A large body of research has been presented on the acoustic energy absorption mechanisms of porous materials [1]. In [2] several of these models are referenced, which, from 1970 to nowadays, have described the acoustic behavior of an absorbing material by means of the characteristic impedance and the propagation constant. In developing these models, the air-flow resistivity is a fundamental magnitude.

The air-flow resistivity and the sound absorption coefficient are part of the acoustic characterization for the marketing of new materials based on natural or recycled fibers [3–5]. These materials are widely used in practical applications in civil engineering and architecture. The air-flow resistivity is also an important parameter in the field of technical textiles. Indeed, specific methods applied to both woven and non-woven textiles of high air-flow resistivity and very low thickness can be found, such as the one proposed by Jaouena & Becot [6]. Formulas for its prediction have also been derived from electronic circuits, as proposed by Pieren [7]. Recent works on the prediction of sound absorption of textiles based on air-flow resistivity, such as that carried out by Tang et al. [8], show that this is also a subject of great interest in the industry.

The air-flow resistivity is the resistance experienced by air while going through a material per thickness unit. It can be obtained either in a laboratory by following the standardized method described in the ISO 9053:2018 standard [9], or by using alternative methods as proposed by different authors [10–13]. Some studies [14] have proposed corrections to the standard to improve the reproducibility between laboratories.

The authors of this work have carried out a recent study on the electroacoustic measurement of the air-flow resistance [15], based on the method described by Dragonetti et al. [13]. In this work, an electroacoustic method for determining the air-flow resistivity, based on the device proposed by Ingard & Dear [11] is presented. Based on the measurement of the total electric impedance of the system (measured at the input terminals of the loudspeaker), the air-flow resistivity is determined using an indirect method.

2. INGARD & DEAR'S METHOD

In 1985, Ingard & Dear presented an acoustic method for the air-flow resistance measurement [11]. In their method, the air-flow resistance is measured by using a cylindrical tube closed with a perfectly rigid termination at one end, a loudspeaker that closes the opposite end, and two measurement microphones. Figure 1 shows a diagram of the measurement device.

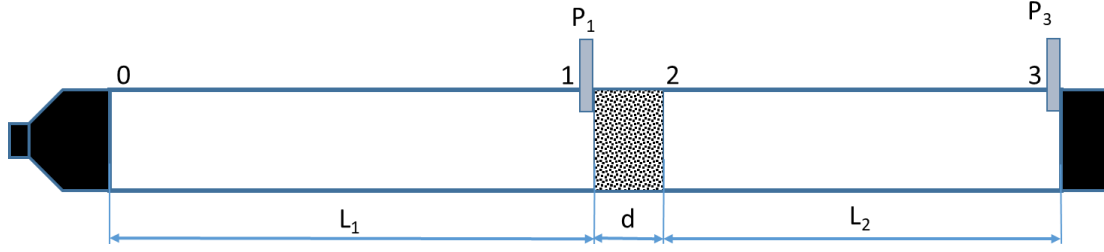


Figure 1. Ingard & Dear's measurement device

The absorbing material, with thickness d , is inserted near the middle of the tube. L_2 is the distance between the rear side of the material and the rigid termination. One of the microphones is placed just at the front of the material sample (P_1), for measuring the sound pressure level at that point. The second microphone is placed at the front of the rigid termination of the tube (P_3) for measuring the sound pressure level at that point. The loudspeaker produces a low-frequency sinusoidal tone, whose frequency is selected with the purpose of generating an odd number of quarter-wavelengths along the $d+L_2$ distance, from the rigid termination to the end of the material sample. This phenomenon occurs at frequencies $f_n = \frac{(2n-1)c_0}{4L_2}$, where n is a natural number and c_0 corresponds to the speed of sound inside the tube. The condition $\lambda \gg 1.7D$ must be met, where λ is the sound wavelength and D is the diameter of the tube.

Considering that losses inside the tube can be neglected, that the microphones are calibrated for having the same sensitivity, and that the flow reactance is small at low frequencies, the air-flow resistance is determined as

$$\sigma = \rho_0 c_0 10^{\frac{(Lp_1 - Lp_3)}{20}}, \quad (1)$$

where ρ_0 is the air mean density in the tube and Lp_1 and Lp_3 are the sound pressure levels corresponding to P_1 and P_3 , respectively.

Equation 1 may be obtained from transfer functions, assuming that losses are negligible:

$$\begin{pmatrix} p_1 \\ U_1 \end{pmatrix} = \begin{pmatrix} 1 & Z_A \\ 0 & 1 \end{pmatrix} \begin{pmatrix} \cos(k_0 L_2) & jZ_0 \sin(k_0 L_2) \\ \frac{j \sin(k_0 L_2)}{Z_0} & \cos(k_0 L_2) \end{pmatrix} \begin{pmatrix} p_3 \\ U_3 \end{pmatrix}, \quad (2)$$

where k_0 is the wave number in the air; U_1 and U_3 are the volume velocities at points P_1 and P_3 , respectively; Z_A is the acoustic impedance of the tested material and Z_0 is the acoustic impedance of air, calculated as $Z_0 = \rho_0 c_0 / S$, where S is the cross-section of the tube.

The rigid wall closing condition ($U_3 = 0$) applied to Equation 2 gives:

$$\begin{pmatrix} p_1 \\ U_1 \end{pmatrix} = \begin{pmatrix} \cos(k_0 L_2) + \frac{jZ_A \sin(k_0 L_2)}{Z_0} & jZ_0 \sin(k_0 L_2) + Z_A \cos(k_0 L_2) \\ \frac{j \sin(k_0 L_2)}{Z_0} & \cos(k_0 L_2) \end{pmatrix} \begin{pmatrix} p_3 \\ 0 \end{pmatrix}$$

$$\begin{pmatrix} p_1 \\ U_1 \end{pmatrix} = \begin{pmatrix} \cos(k_0 L_2) + \frac{jZ_A \sin(k_0 L_2)}{Z_0} \\ \frac{j \sin(k_0 L_2)}{Z_0} \end{pmatrix} p_3 \quad . \quad (3)$$

From Equation 3, Ingard & Dear's equation is obtained as

$$\frac{p_1}{p_3} = \cos(k_0 L_2) + \frac{jZ_A \sin(k_0 L_2)}{Z_0},$$

and Z_A can be obtained

$$Z_A = -jZ_0 \left(\frac{p_1}{p_3} \frac{1}{\sin(k_0 L_2)} - \cot(k_0 L_2) \right). \quad (4)$$

As described in the work by Ingard & Dear, Equation 4 can be simplified for frequencies where the cotangent is canceled ($f_n = \frac{(2n-1)c_0}{4L_2}$, where n is a natural number), and Z_A is given by

$$Z_A = \mp jZ_0 \frac{p_1}{p_3}. \quad (5)$$

From Equation 5, the normalized flow resistance (σ) is obtained:

$$\sigma = \left| \text{Im} \frac{p_1}{p_3} \right|. \quad (6)$$

Equation 1 is then obtained from Equation 6. In [2], a comparison between this method and other two approaches has been reported.

3. THE PROPOSED ELECTROACOUSTIC MODEL

3.1. Electroacoustic transformation

The proposed electroacoustic transformation is similar to the one described in Alba et al. [15]. The total electric impedance of the setup described in Figure 1, Z_{ET} , can be obtained as

$$Z_{ET} = Z_E + Z_{MOV} = Z_E + \frac{(Bl)^2}{Z_{AT} \cdot S^2}, \quad (7)$$

$$Z_E = R_E + j\omega L_E. \quad (8)$$

In Equations 7 and 8, Z_E is the pure electric impedance of the loudspeaker, where R_E is the electric resistance of the voice coil and L_E is the voice-coil inductance, S is the cross-sectional area of the tube, Bl is the electromagnetic coupling constant of the loudspeaker and Z_{AT} is the total acoustic impedance of the system. In this case, Z_{AT} is the load over the loudspeaker plus the effect of the mechanical impedance of the loudspeaker, Z_M , given by

$$Z_{ET} = Z_E + \frac{(Bl)^2}{Z_M + Z_{A0} S^2}. \quad (9)$$

3.2. System without the sample

In the case of the empty tube with length L ($L = L_1 + L_2 + d$), the impedance at P_1 can be used as a reference. From Equation 3, with $Z_A = 0$, Z_{A1} can be obtained as

$$Z_{A1} = \frac{p_1}{U_1} = \frac{\cos(k_0 L)}{\frac{j \sin(k_0 L)}{Z_0}} = -jZ_0 \cotg(k_0 L). \quad (10)$$

Equation 10 is the classical equation for an empty tube without losses [16]. In this case, we have that

$$Z_{ET} = Z_E + \frac{(Bl)^2}{Z_M - jZ_0 \cotg(k_0 L) S^2}. \quad (11)$$

Equation 11 can be used to calibrate the system, both the mechanical impedance of the loudspeaker and the length of the tube. We note that when the cotangent of the denominator cancels then $f_n = \frac{(2n-1)c_0}{4L}$, with n a natural number.

3.3. System with the test sample

When the test sample is introduced in the tube (see Figure 1), the total electric impedance is determined by

$$\begin{pmatrix} p_0 \\ U_0 \end{pmatrix} = \begin{pmatrix} \cos(k_0 L_1) & jZ_0 \sin(k_0 L_1) \\ \frac{j \sin(k_0 L_1)}{Z_0} & \cos(k_0 L_1) \end{pmatrix} \begin{pmatrix} 1 & Z_A \\ 0 & 1 \end{pmatrix} \begin{pmatrix} \cos(k_0 L_2) & jZ_0 \sin(k_0 L_2) \\ \frac{j \sin(k_0 L_2)}{Z_0} & \cos(k_0 L_2) \end{pmatrix} \begin{pmatrix} p_3 \\ U_3 \end{pmatrix},$$

and Z_{A0} is obtained as

$$Z_{A0} = \frac{p_0}{U_0} = -jZ_0 \frac{\cos(k_0(L_1 + L_2)) + \frac{jZ_A}{Z_0} \cos(k_0 L_1) \sin(k_0 L_2)}{\sin(k_0(L_1 + L_2)) + \frac{jZ_A}{Z_0} \sin(k_0 L_1) \sin(k_0 L_2)}. \quad (12)$$

In Equation 12 we obtain those particular cases where cotangent cancels (i.e., $f_n = \frac{(2n-1)c_0}{4L}$, with n a natural number): $\cos(k_0 L_1) = 0$ and ($\sin(k_0 L_1) = \pm 1$), so

$$Z_{A0} = -jZ_0 \frac{\pm \sin(k_0 L_2)}{\pm \cos(k_0 L_2) \pm \frac{jZ_A}{Z_0} \sin(k_0 L_2)} = \frac{Z_0}{j \cotg(k_0 L_2) - \frac{Z_A}{Z_0}}. \quad (13)$$

if $L_1 = L_2$ Equation 13 is

$$Z_{A0} = -\frac{Z_0^2}{Z_A}. \quad (14)$$

Therefore, in this case we have that

$$Z_{ET} = Z_E + \frac{(Bl)^2}{Z_M - \frac{Z_0^2}{Z_A}}. \quad (15)$$

4. EXPERIMENTAL RESULTS

4.1 Calibration

Figure 2 shows the actual setup, where $L_1 = 89.1$ cm and $L_2 = 85$ cm. The tube diameter is 4.2 cm.

For calibrating the system, a measurement is performed when the loudspeaker is mechanically-loaded by the empty tube of length L_1 terminated with a rigid end (Figure 3). Figure 4 shows the results of the measurement of the real and imaginary parts of the total electric impedance are presented as a function of frequency. Figure 5 shows the corresponding total mechanical impedance of the system. Under these conditions, the

frequencies that satisfy $f_n = \frac{(2n-1)c_0}{4L_1}$, with $c_0 = 345$ m/s, are: 96.8 Hz, 290.4 Hz, 484.0 Hz, 676.6 Hz, etc. At these frequencies, Equation 11 is given by

$$Z_{ET} = Z_E + \frac{(Bl)^2}{Z_M}$$

Using $Bl = 15$ N/A, as given by the loudspeaker's manufacturer, the values of Z_M at these frequencies can be obtained and then used for the calibration of the device. In the case of the second harmonic, $Z_M = 27.14 - j39.83 \Omega_{\text{mec}}$.

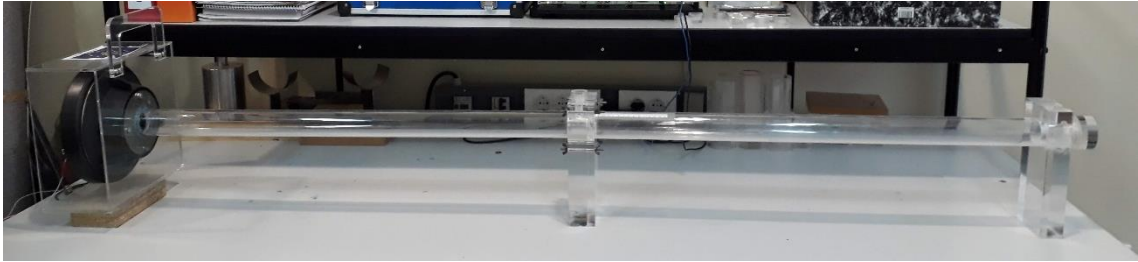


Figure 2. Experimental setup showing the full tube

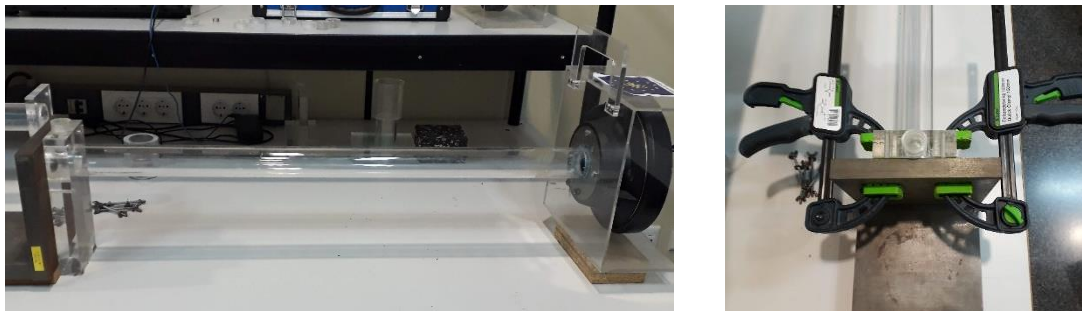


Figure 3. System with the closed-end tube of length L_1

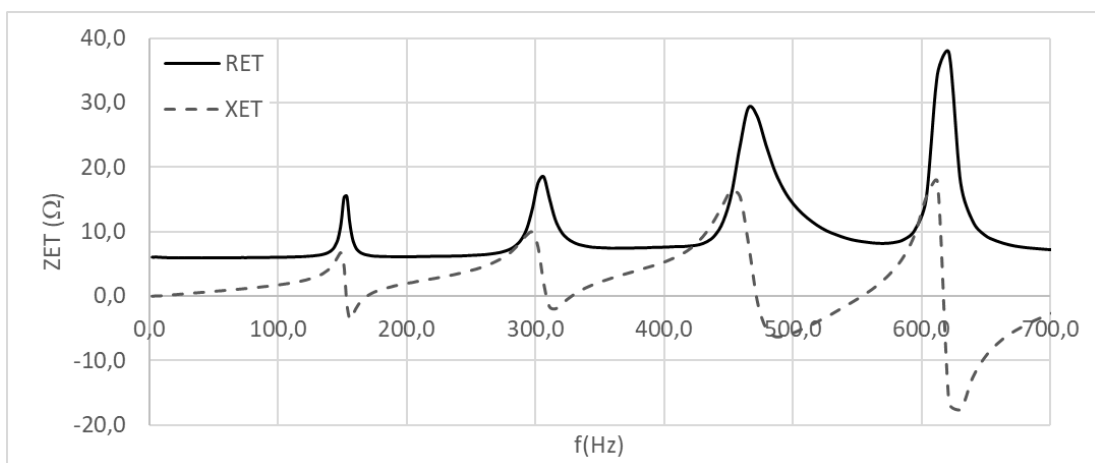


Figure 4. Measurement of the total electric impedance with tube in Figure 3

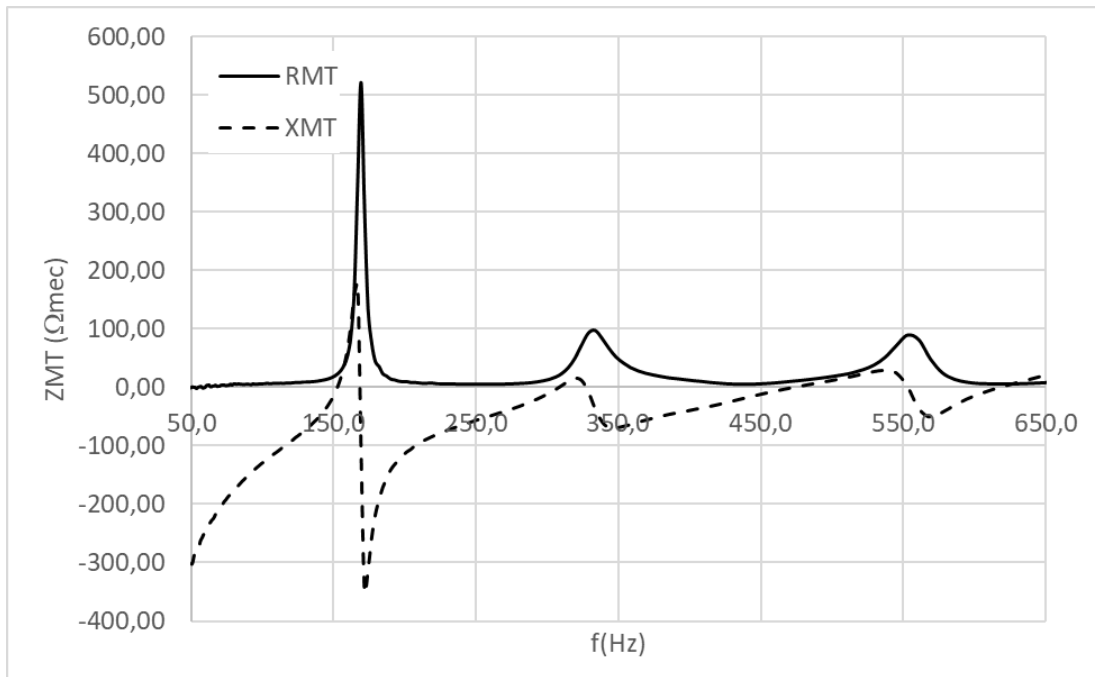


Figure 5. Total mechanical impedance with tube in Figure 3

4.2 Measurement of material samples

To test the device a set of nine material samples were measured. These materials were Polyester-based (I400-30, I400-40), made of coconut fibers (coco1, coco2, coco3), recycled foams (D80 and D150) and cork samples (corcho2, corcho3). These materials are similar to those studied in previous works [1,15,17–19].

Figure 6 shows an example of the total electric impedance obtained for the I400-30 material and the corresponding mechanical impedance is presented in Figure 7.

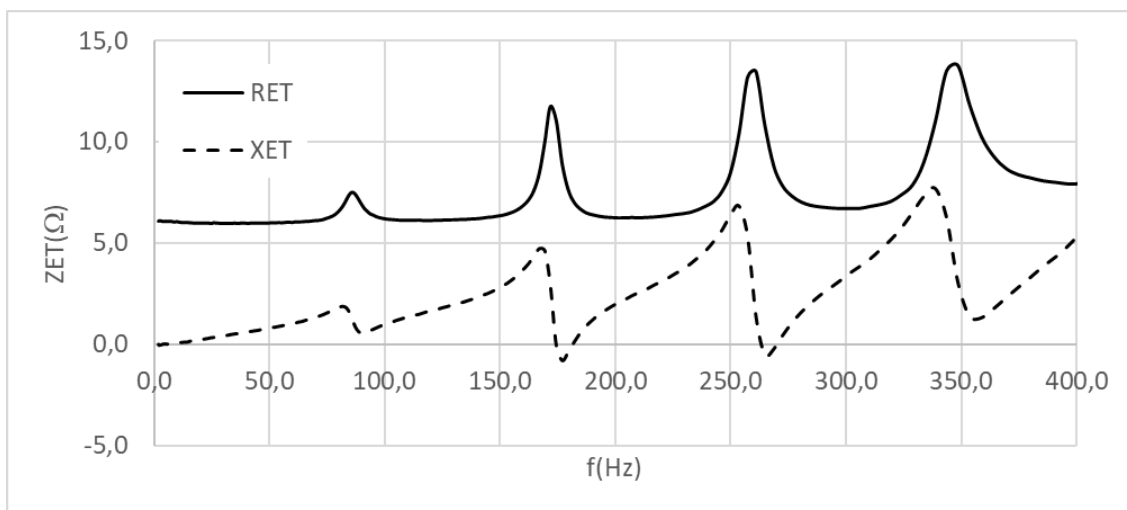


Figure 6. Total electric impedance measured with a sample of I400-30

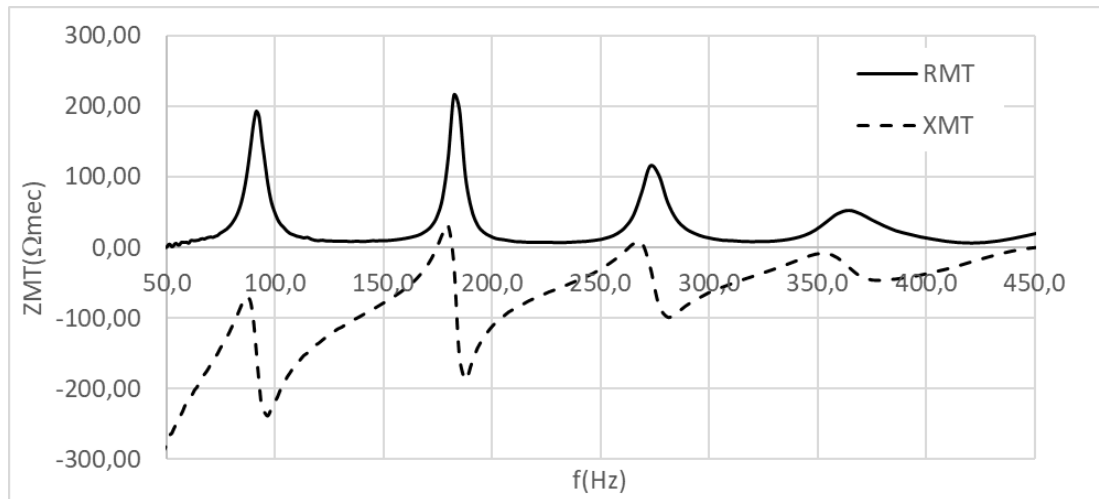


Figure 7. Total mechanical impedance measured with a sample of I400-30

Table 1 summarizes the results obtained for all materials, taking 290.4 Hz as the reference frequency, where the curves are stables. Results have been obtained using Equation 15, considering the calibration process, and assuming that L_1 and L_2 are similar.

Table 1. Results of specific air-flow resistivity

MATERIAL	Density (kg/m³)	Thickness (cm)	Airflow resistance (Ns/m³)	σ (Ns/m⁴)
I400-30	14	3,3	50 ± 1	1500 ± 80
I400-40	10	3,9	53 ± 3	1340 ± 50
coco1	125	2,4	51 ± 1	2160 ± 40
coco2	100	2,9	52 ± 2	1750 ± 50
coco3	73	5,2	50 ± 1	950 ± 40
corcho2	140	2	650 ± 6	32400 ± 300
corcho3	156	3	720 ± 200	24000 ± 6500
D80	90	3,5	281 ± 12	8100 ± 350
D150	192	3,3	1300 ± 170	29700 ± 5700

Corresponding results obtained for materials labelled as I400-30 and I400-40 can be found in [15]. Standardized values using the ISO-9053 are 1500 and 1100 Ns/m⁴, respectively. Air-flow resistivity measurements for the material labelled as coco2 were presented in [15] reporting a value of 1900 Ns/m⁴. Results presented in Table 1 are coherent and very similar to those obtained by following the ISO 9053 standard.

4. CONCLUSIONS

In this work, an alternative method for the measurement of air-flow resistivity of porous materials has been presented. It is based on the electroacoustic analysis of the Ingard & Dear's device. After a straightforward calibration, the air-flow resistance is obtained from the measurement of the total electric impedance. The proposed method is simple and does not require complex instrumentation, so it could be considered an inexpensive alternative for the determination of this parameter. Experimental tests using the proposed method were very similar to those obtained using the ISO standard, and reported a very low deviation.

5. ACKNOWLEDGEMENTS

The authors would like to gratefully acknowledge the support of CONICYT-FONDECYT under Grant 1171110.

6. REFERENCES

1. Arenas, J. P.; Crocker, M. J. Recent Trends in Porous Sound-Absorbing Materials. *Sound Vib.* **2010**, *44* (7), 12–17.
2. Rey, R. del; Alba, J.; Arenas, J. P.; Ramis, J. Technical Notes: Evaluation of Two Alternative Procedures for Measuring Airflow Resistance of Sound Absorbing Materials. *Arch. of Acoust.* **2013**, *38* (4), 547–554. <https://doi.org/10.2478/aoa-2013-0064>.
3. Maderuelo-Sanz, R.; Nadal-Gisbert, A. V.; Crespo-Amorós, J. E.; Parres-García, F. A Novel Sound Absorber with Recycled Fibers Coming from End of Life Tires (ELTs). *Appl. Acoust.* **2012**, *73* (4), 402–408. <https://doi.org/10.1016/j.apacoust.2011.12.001>.
4. Ekici, B.; Kentli, A.; Küçük, H. Improving Sound Absorption Property of Polyurethane Foams by Adding Tea-Leaf Fibers. *Arch. of Acoust.* **2012**, *37* (4), 515–520. <https://doi.org/10.2478/v10168-012-0052-1>.
5. Garai, M.; Pompoli, F. A Simple Empirical Model of Polyester Fibre Materials for Acoustical Applications. *Appl. Acoust.* **2005**, *66* (12), 1383–1398. <https://doi.org/10.1016/J.APACOUST.2005.04.008>.
6. Jaouen, L.; Bécot, F.-X. Acoustical Characterization of Perforated Facings. *J. Acoust. Soc. Am.* **2011**, *129* (3), 1400–1406. <https://doi.org/10.1121/1.3552887>.
7. Pieren, R. Sound Absorption Modeling of Thin Woven Fabrics Backed by an Air Cavity. *Text. Res. J.* **2012**, *82* (9), 864–874. <https://doi.org/10.1177/0040517511429604>.
8. Tang, X.; Jeong, C.-H.; Yan, X. Prediction of Sound Absorption Based on Specific Airflow Resistance and Air Permeability of Textiles. *J. Acoust. Soc. Am.* **2018**, *144* (2), EL100–EL104. <https://doi.org/10.1121/1.5049708>.
9. *ISO 9053-1:2018. Acoustics. Determination of Airflow Resistance -- Part 1: Static Airflow Method*; 2018.
10. Stinson, M. R.; Daigle, G. A. Electronic System for the Measurement of Flow Resistance. *J. Acoust. Soc. Am.* **1988**, *83* (6), 2422–2428. <https://doi.org/10.1121/1.396321>.
11. Ingard, K. U.; Dear, T. A. Measurement of Acoustic Flow Resistance. *J. Sound Vib.* **1985**, *103* (4), 567–572. [https://doi.org/10.1016/S0022-460X\(85\)80024-9](https://doi.org/10.1016/S0022-460X(85)80024-9).
12. Ren, M.; Jacobsen, F. A Method of Measuring the Dynamic Flow Resistance and Reactance of Porous Materials. *Appl. Acoust.* **1993**, *39* (4), 265–276.

- [https://doi.org/10.1016/0003-682X\(93\)90010-4](https://doi.org/10.1016/0003-682X(93)90010-4).
13. Dragonetti, R.; Ianniello, C.; Romano, R. A. Measurement of the Resistivity of Porous Materials with an Alternating Air-Flow Method. *J. Acoust. Soc. Am.* **2011**, *129* (2), 753–764. <https://doi.org/10.1121/1.3523433>.
 14. Garai, M.; Pompoli, F. A European Inter-Laboratory Test of Airflow Resistivity Measurements. *Acta Acust. united with Acust.* **2003**, *89*, 471–478.
 15. Alba, J.; Arenas, J. P.; del Rey, R.; Rodríguez, J. C. An Electroacoustic Method for Measuring Airflow Resistivity of Porous Sound-Absorbing Materials. *Appl. Acoust.* **2019**, *150*, 132–137. <https://doi.org/10.1016/J.APACOUST.2019.02.009>.
 16. Kinsler, L. E. *Fundamentals of Acoustics*; Wiley, 2000.
 17. Del Rey, R.; Alba, J.; Ramis, J.; Sanchís, V. J.; Sanchís, V. J. New Absorbent Acoustic Materials from Plastic Bottle Remnants. *Mater. Construcción* **2011**, *61* (304), 547–558. <https://doi.org/10.3989/mc.2011.59610>.
 18. Rey, R. del; Alba, J.; Arenas, J. P.; Sanchis, V. J. An Empirical Modelling of Porous Sound Absorbing Materials Made of Recycled Foam. *Appl. Acoust.* **2012**, *73* (6–7), 604–609. <https://doi.org/10.1016/J.APACOUST.2011.12.009>.
 19. Ramis, J.; Del Rey, R.; Alba, J.; Godinho, L.; Carbajo, J. A Model for Acoustic Absorbent Materials Derived from Coconut Fiber. *Mater. Construcción* **2014**, *64* (313), e008. <https://doi.org/10.3989/mc.2014.00513>.